

## Detection of Quiescent Phases in Echocardiography Data using Non-Linear Filtering and Boundary Detection

Lakshminarayan Ravichandran, Carson A. Wick, *IEEE Student Member*,  
and Srini Tridandapani, *IEEE Member*

**Abstract**—In order to detect the quasi-stationary states of the heart within a cardiac cycle from echocardiography data, we present an algorithm that uses non-linear filtering and boundary detection. The non-linear filtering algorithm involves anisotropic diffusion to remove the speckle noise from the data and to smoothen the homogeneous regions while preserving the edges. Following this, we perform binary thresholding and boundary detection, and observe the positional changes in the region of interest. From a series of echocardiography images, we derived the regions of cardiac quiescence, which we then plotted on the electrocardiograph (ECG) R–R interval. It is observed that the quiescence occurs in the diastolic region of the ECG signal, but the position and length of quiescence varies across multiple cardiac cycles for the same individual.

### I. INTRODUCTION

Cardiac computed tomography (CT) evaluation of the coronary arteries is at the cusp of revolutionizing diagnosis of heart disease. CT evaluation is fast, inexpensive, and noninvasive and has relatively rare complications compared with the more invasive and expensive catheter-based coronary angiography. However, CT evaluation of the heart has a fundamental drawback in the form of temporal resolution. CT gantry rotation times are of the order of 330ms and slice acquisition times are about 170ms for current single-source CT scanners. On the other hand, the heart is a moving target, which makes acquisition of motion-free images challenging. There are, however, portions of the cardiac cycle where the heart is relatively quiescent, and scanning during these periods may reduce motion artifacts. For example, if the heart rate is below 70 beats per minute (bpm), then CT slice acquisition in the diastolic portion of the cardiac cycle may provide relatively motion-free images of the coronary arteries, and if the heart rate is greater than 70bpm, then scanning in the systolic portion of the cycle may be better [1].

Currently, prediction of cardiac quiescence is based almost-entirely on electrocardiography (ECG), and CT slice acquisition is based on a gating signal that is derived from real-time ECG. ECG is an excellent marker of the instantaneous electrical state of the heart; however, it is not a great

marker of the instantaneous mechanical motion of the heart. Our hypothesis is that cardiac CT gating can be improved if the gating signal is based on the true mechanical motion of the heart rather than the surrogate electrical marker.

In prior work [2], we have shown that ultrasound (US), which, similar to ECG, can provide real-time evaluation of the heart, may potentially provide a better signal for gating since it directly interrogates cardiac mechanical motion. In that work, we showed that quiescent periods within the cardiac cycle may vary between individuals even if their heart rates are similar. Thus ECG gating at fixed interval within the cardiac cycle may not be optimal using population-derived averages.

A limitation of the work in [2] was that it was based on beat-to-beat cross-correlation of one-dimensional (M-mode) US signals from the left ventricular wall. M-mode can only resolve motion in one direction at a time and motion in the orthogonal direction cannot be resolved. In this paper, estimation of cardiac quiescence is performed by observing the motion of the inter-ventricular septum in a series of two-dimensional (B-mode) US images.

The B-mode US image is a two-dimensional depiction of the echoes plotted as a function of depth. However, speckle noise is usually associated with this imaging modality, which can hamper edge detection and image segmentation. The cardiac quiescence estimation algorithm in this paper performs despeckling of the ultrasound image using a non-linear filtering technique called anisotropic diffusion (AD), which also performs contrast enhancement and edge detection. Using this filtered image, the boundary around the region of interest (ROI), also referred to as object contour, is obtained and the center of mass of the ROI is calculated. This center of mass can be considered to represent the position of the ROI in that particular frame. This process is repeated over the entire set of US data and an estimate of the position of the ROI over multiple frames is thus obtained. We then compare the motion estimates obtained by this approach with the simultaneously and synchronously acquired ECG signal.

The rest of this paper is organized as follows: In Section II, our mathematical techniques for processing the US cine data are presented. In Section III, our experimental setup and results of the evaluation of our algorithm based on data from two human subjects are provided. Finally, Section IV provides a discussion and the conclusions.

The project described was supported by Award Number K23EB013221 from the National Institute of Biomedical Imaging and Bioengineering. The content is solely the responsibility of the authors and does not necessarily represent the official views of the National Institute of Biomedical Imaging and Bioengineering or the National Institutes of Health. L. Ravichandran and S. Tridandapani are with the Department of Radiology and Imaging Sciences, Emory University School of Medicine, Atlanta, GA 30322 USA. (e-mail: lravich@emory.edu, stridan@emory.edu). C. A. Wick is with the School of Electrical and Computer Engineering, Georgia Institute of Technology, Atlanta, GA 30332 USA (e-mail: carson@gatech.edu).

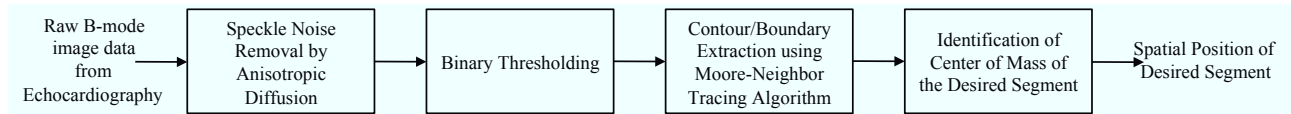


Fig. 1. Block diagram: cardiac quiescence detection using anisotropic diffusion and boundary detection.

## II. METHODS

In this section, we describe the steps involved in the detection of cardiac quiescence from B-mode US data, as outlined in Fig. 1.

### A. Anisotropic Diffusion

In order to segment the image into a pre-specified ROI and to perform tracking, we initially use a filtering algorithm to remove the speckle noise. Speckle noise is a result of the interference of ultrasound waves while gathering back-scattered data. Speckle causes distortions in the image that can seriously hamper the detection of the ROI. In order to be able to detect the motion from this ultrasound image, we need to suppress the speckle noise, and this can both enhance the contrast of the image and enable better edge and boundary detection of the ROI. There are many linear and non-linear filtering techniques including averaging filters, Wiener filters, Lee filter, Frost filter and anisotropic diffusion based filters [3] that have been used to remove speckle noise in US. While the Wiener, Lee and Frost filters remove speckle noise, the despeckled images lose important edge details due to smoothing, and these edge details are important in the detection of ROI. In this algorithm we use the anisotropic diffusion (AD) filter originally proposed in [4] which was modified for medical images in [5], [6]. We use the AD filter since it performs smoothing based on the gradient of the image intensity, and provides an edge enhanced and contrast enhanced image while removing the speckle noise.

The following mathematical framework for the AD algorithm follows the approach presented by Gerig et al. in [5]. For a vector  $\bar{x}$  which represents the spatial co-ordinates and  $t$ , the process ordering parameter, the process of smoothing via diffusion is given by:

$$\frac{\partial}{\partial t} u(\bar{x}, t) = \text{div}(c(\bar{x}, t) \nabla u(\bar{x}, t)) \quad (1)$$

where  $c(\bar{x}, t)$  is the diffusion function that depends on the magnitude of the gradient of the image intensity  $I(\bar{x}, t) = u(\bar{x}, t)$ . The diffusion function used in this algorithm is obtained as a function of the image intensity and is given by:

$$c(\bar{x}, t) = \left( 1 + \left( \frac{|\nabla I(\bar{x}, t)|}{\kappa} \right)^2 \right)^{-1} \quad (2)$$

This diffusion function is a monotonically decreasing function which diffuses within the regions leaving the boundaries (high gradient regions) unaffected. The diffusion process continues until the gradient reaches a large value, i.e. discontinuity occurs. The parameter  $\kappa$  depends on the noise level and the edge strength.

The two-dimensional implementation of the AD filtering ( $\bar{x} = [x \ y]$ ) for an image with intensity  $I(\bar{x}, t)$  is given by:

$$\begin{aligned} \frac{\partial}{\partial t} I(\bar{x}, t) &= \text{div}[c(\bar{x}, t) * \nabla I(\bar{x}, t)] \\ &= \frac{\partial}{\partial x} \left[ c(\bar{x}, t) * \frac{\partial}{\partial x} I(\bar{x}, t) \right] \\ &\quad + \frac{\partial}{\partial y} \left[ c(\bar{x}, t) * \frac{\partial}{\partial y} I(\bar{x}, t) \right] \end{aligned}$$

This diffusion is calculated in the neighboring pixel directions, and the updated pixel intensity is given by:

$$I(\bar{x}, t + \Delta t) = I(\bar{x}, t) + \Delta t * \frac{\partial}{\partial t} I(\bar{x}, t) \quad (3)$$

where  $\Delta t$  is the integration constant and is used to approximate the stability. Since this algorithm does not have a specific convergence, that is, the smoothing continues to occur up to infinite time, a constraint on the number of iterations is imposed. The number of iterations depends on the application and the amount of smoothing desired.

This process of AD blurs smaller discontinuities and sharpens the edges, which is useful in this despeckling process, while retaining the discontinuities and not affecting their positions. We refer to this anisotropic diffused image as  $I_{AD}(\bar{x}, t)$  or simply  $I_{AD}$ .

### B. Thresholding

Following the removal of the speckle noise, which also enhances the contrast of the image while enabling edge detection, we perform a hard thresholding on the image  $I_{AD}$  in order to be able to better identify the contour of the ROI. This is a binary thresholding process with the value for the threshold obtained by the separation between the hyperechoic (higher pixel intensity) and the hypoechoic region (lower pixel intensity) of the histogram despeckled image. Due to AD filtering, there is enhancement of contrast, thus widening the separation between the hypoechoic and the hyperechoic regions in the histogram. The pixel values greater than the threshold are set to one (white), and the ones below the threshold are set to zero (black)

### C. Boundary Detection

On the binary image obtained after thresholding, we perform the boundary detection using the Moore neighbor algorithm modified by Jacob's stopping criteria [7]. The boundary detection algorithm delineates the contour of the ROI and the points within the contour. Using these points, we find the center of the mass  $(c_{x_i}, c_{y_i})$ , for the ROI for frame  $i$ .

The above process of finding the ROI, corresponding to the part of the heart whose motion we are tracking, and the center of of mass for this ROI, is repeated over the entire set of frames. This results in the vector  $\mathbf{C}$  that provides the position of the ROI for each of the frames from which the quiescence is computed.

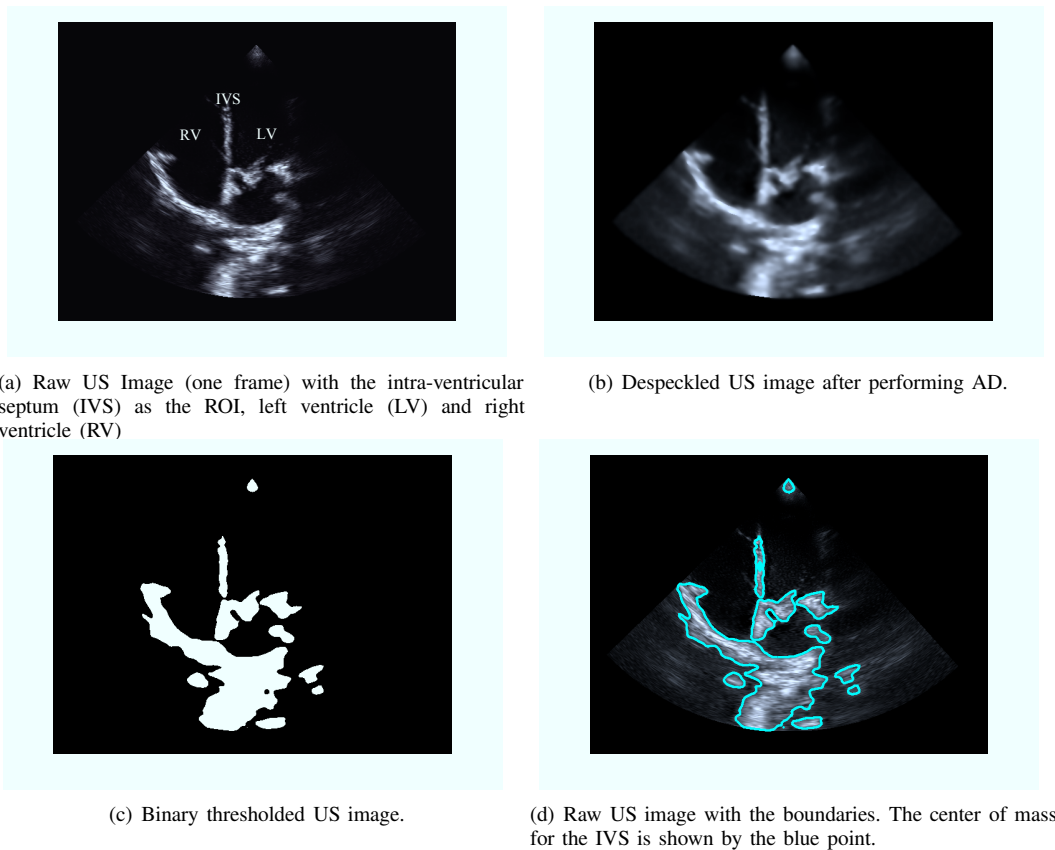


Fig. 2. Illustration of detection of center of mass of the septum for a frame of B-mode echocardiograph data.

#### D. Motion

The position vector  $\mathbf{C} = [C_1; C_2; \dots; C_N]$ , where  $C_i = (c_{x_i}, c_{y_i})$  and  $N$  is the number of frames, is used to compute the motion of the ROI over the entire set of frames. In order to observe quiescence, i.e. the region of no motion, the position of two consecutive frames needs to be compared. In order to achieve this, we consider the first difference between the  $x$  and the  $y$  positions of consecutive frames. i.e.,  $\Delta C_i = C_{i+1} - C_i$

We then observe the regions where the first difference for both the  $x$  and  $y$  position is close to zero. The longer the stretch of zeros in the first difference, the longer the region of quiescence.

### III. EXPERIMENTAL SETUP AND RESULTS

The experimental data is obtained using a SonixTOUCH Research ultrasound machine (Ultrasonix, Vancouver, BC, Canada), and the data consists of the B-mode echocardiography images and ECG data for two female subjects of ages 23 and 24 (subject A and B, respectively), with no known cardiac conditions. Approval for the study was obtained from the Institutional Review Board (IRB) at Emory University. The data acquisition rate of the B-mode echocardiography data is 30 frames/sec and that for the ECG data is 200 samples/sec. The size of a single echocardiography data frame is  $640 \times 480$ . The algorithm was evaluated on MATLAB v7.10 (MathWorks Inc., Natick, MA).

To evaluate the cardiac quiescence algorithm described in Section II, we consider B-mode echocardiography data and ECG data. For the AD filtering, the gradient modulus threshold parameter  $\kappa$  is set to 30 and the number of iterations for smoothing was set to 10. These values for  $\kappa$  and the number of iterations were set upon observing the gradient of the US image and the desired despeckling. It was observed that 10 iterations were sufficient to remove the speckle noise and enhance the contrast. For the hard thresholding process following the AD filtering, the threshold was determined from the histogram and was set to 50. Note that this threshold can vary with the brightness and the contrast of image acquired and following the AD filtering process.

In Fig. 2, the algorithm steps are illustrated for a B-mode echocardiography image of the subject, and we desire to detect the center of mass of the septum. Note that in this case, the boundary detection is performed over the entire image. It suffices if it is performed over a roughly estimated area containing the region of interest rather than the entire image. Fig. 2(a) shows the raw image upon which AD filtering was performed to obtain the image shown in Fig. 2(b). Fig. 2(c) shows the binary thresholded image after AD filtering upon which the boundary detection is performed, and the detected boundaries are shown on the raw ultrasound image in Fig. 2(d) along with the center of mass of the septum.

Upon obtaining the centers of mass  $\mathbf{C}$  for the septum for the entire set of frames, we find the first difference  $\Delta \mathbf{C}$  from

C. This first difference can also be interpreted as the velocity in the  $x$  and  $y$  directions. We then observe the regions of low (close to zero) first difference of both  $x$  and  $y$  positions, which implies that there has been very little or no motion (first difference between consecutive frame less than 0.2cm) with respect to the consecutive frames of B-mode. The region of quiescence is then drawn over the ECG signal that is obtained at the same time as the B-mode data.

From the aforementioned data sets, we initially show results for subject B for an average heart rate of 65 bpm. The first difference of the  $x$  and  $y$  position of the septum  $\Delta C = [\Delta x \ \Delta y]$ , the ECG signal and the region of quiescence as obtained from analyzing the B-mode data is shown for a segment of the data (three cardiac cycles) in Fig. 3.

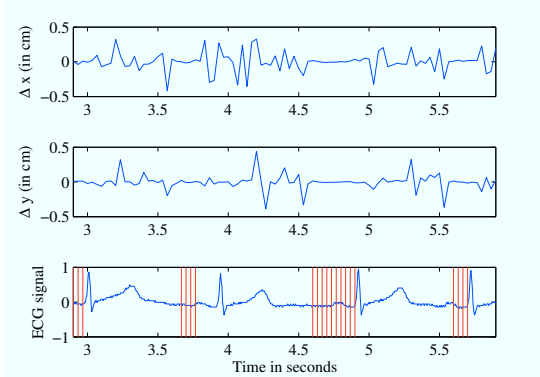


Fig. 3. Plot of first difference of  $x$  and  $y$  positions ( $\Delta x$  and  $\Delta y$ ) and the ECG signal with the cardiac quiescence shown by red bars.

Note that the quiescence is shown by red bars and is observed over the diastolic portion of the cardiac cycle. For the three cardiac cycles shown (of durations 0.93s, 0.91s, and 0.8s), we see that the quiescence begins at a different point in each cardiac cycle and the quiescence is of different durations. For example, a longer duration of quiescence is observed for the second cardiac cycle, while the quiescence in the third cardiac cycle occurs at a later point when compared to the other two cycles.

Thus, we see that the region of quiescence may vary with the length of the cardiac cycle for the same patient. In order to further investigate this finding, we consider 10 cardiac cycles of different lengths drawn from subject A and B, both with an average heart rate 55. For each of the cardiac cycles, we consider the region of quiescence in the diastolic region, and obtain the quiescence start and end points as a percentage with respect to the duration of the cardiac cycle. This is shown in Fig. 4 where the normalized quiescence start and end points are plotted for each of the cardiac cycles. Note that the start of quiescence varies between 60–80% of the cardiac cycle length and the quiescence duration can extend between 10–35% of the cardiac cycle length.

#### IV. DISCUSSION AND CONCLUSION

Using AD, binary thresholding and boundary detection, we were able to identify the motion of the septum from B-mode US data for gating purposes. The identification of the region of quiescence with reference to the ECG signal acquired simultaneously showcased the following findings.

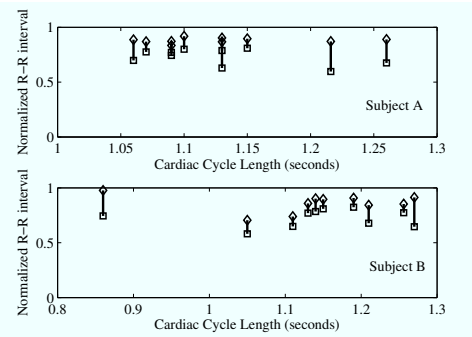


Fig. 4. Cardiac quiescence start and end points for Subject A and B are plotted for 10 cardiac cycles as a percentage of the cardiac cycle length against the cardiac cycle duration.

For heart rates in the range 55–65bpm, the quiescent region is observed in the diastolic portion of the cardiac cycle. However, this cardiac quiescence state is not deterministic, i.e. its exact position and duration on a beat-to-beat basis cannot be determined given the cardiac cycle duration or the heart rate. The quiescence position and duration is also shown to vary within the same individual for different cardiac cycle duration and also across two different individuals.

Future work will focus on observing the quiescence over a larger range of heart rates for the same subject and determining if there is any quiescence detected by this algorithm in the the systolic region of the cardiac cycle for higher heart rates. In addition, the correlation between the motion from different ROI for the same set of frames will be computed, to study if quiescence occurs simultaneously or with a delay, on all parts of the left ventricle and eventually the other regions of the heart. Additionally, we would like to retain speckle noise and observe if tracking this speckle noise enables better motion analysis and quiescence prediction.

Ultimately we would like to develop algorithms using a non-linear filtering approach to model cardiac motion and predict quiescence. This will permit optimal gating for cardiac CT examinations.

#### ACKNOWLEDGMENTS

The authors would like to thank Siddhartha Datta Roy from Georgia Institute of Technology for help with the software on the SonixTOUCH ultrasound machine.

#### REFERENCES

- [1] J. P. Earls *et al.*, “Prospectively Gated Transverse Coronary CT Angiography versus Retrospectively Gated Helical Technique: Improved Image Quality and Reduced Radiation Dose,” *Radiology*, vol. 246, no. 3, pp. 742–753, March 2008.
- [2] S. Tridandapani, J. B. Fowlkes, and J. M. Rubin, “Echocardiography-based Selection of Quiescent Heart Phases,” *J. of Ultrasound in Medicine*, vol. 24, no. 11, pp. 1519–1526, 2005.
- [3] P. Tay *et al.*, “Ultrasound Despeckling for Contrast Enhancement,” *IEEE Trans. on Image Proc.*, vol. 19, no. 7, pp. 1847–1860, July 2010.
- [4] P. Perona and J. Malik, “Scale-Space and Edge Detection Using Anisotropic Diffusion,” *IEEE Trans. on Pattern Analysis and Machine Intelligence*, vol. 12, no. 7, pp. 629–639, July 1990.
- [5] G. Gerig *et al.*, “Nonlinear Anisotropic Filtering of MRI Data,” *IEEE Trans. on Medical Imaging*, vol. 11, no. 2, pp. 221–232, Jun 1992.
- [6] Y. Yu and S. Acton, “Speckle Reducing Anisotropic Diffusion,” *IEEE Trans. on Image Proc.*, vol. 11, no. 11, pp. 1260–1270, Nov 2002.
- [7] R. C. Gonzalez, R. E. Woods, and S. L. Eddins, *Digital Image Processing Using MATLAB*. Pearson Prentice Hall, 2004.